

Study of optical properties of vacuum evaporated $\text{Ge}_{1-x}\text{Sn}_x\text{Se}_{2.5}$ ($x=0, 0.3, 0.5$) thin films

DEEPIKA^{a,*}, H. SINGH^a, N. S. SAXENA^b

^aDept. of Applied Sciences, The NorthCap University, Sector 23 -A, Gurugram, India

^bSemiconductor and Polymer Science Lab., Dept. of Physics, University of Rajasthan, Jaipur, India

Optical properties of $\text{Ge}_{1-x}\text{Sn}_x\text{Se}_{2.5}$ ($x=0, 0.3, 0.5$) thin films have been studied using absorption and transmission spectra in range 400–1200 nm. Thermal evaporation technique has been used to deposit films onto cleaned glass substrate. Energy band gap has been determined using the absorption spectra while transmission spectra have been used to obtain refractive index and thickness of the films using the method proposed by Swanepoel. Other optical parameters i.e., extinction coefficients, band tail width, dielectric constant has also been evaluated. The studies show that refractive index increases while the band gap decreases with increase in Sn concentration.

(Received June 7, 2018; accepted February 12, 2019)

Keywords: Chalcogenides, Glasses, Vacuum deposition, Thin films, Energy band gap

1. Introduction

Chalcogenide glasses have been endorsing a great deal of interest in the past decades due to their large applications in electrical and optical memory devices, opto-electronics, optical fibres, xerography, infra-red lenses, electro-photography solar cells etc. [1-6]. These glasses have tunable band gap which can be varied with composition of constituent alloys. Beside this, these glasses also show high transmittance in far-infrared region, due to which they find application in fabrication of optical devices [7-8]. Chalcogenide semiconductor materials are dispersive in nature, therefore their refractive index depend on wavelength [9]. The variation in values of refractive index (real and imaginary) with wavelength and thickness provides important information for use of material in opto-electronic devices [10-11]. Thermally evaporated thin films of chalcogenide semiconductors have found applications in vast areas such as display devices, optical amplifiers and optical recording media [12-14]. Germanium–selenium glass system is of interest due to its good glass forming ability and its application in fabrication of optical fibers and recording devices [15–19]. In the Ge–Se system, Ge atoms form bonds with Se chains thereby increasing the average bond strength of the system [20]. When third element is added to the Ge–Se system, it is expected to create compositional and conformational disorder in the system. This consequently leads to new bond formations and structural rearrangement of the system. Therefore, addition of Sn in Ge–Se system is expected to enhance the glass forming ability of Ge–Se system [21-22].

In the present communication, optical parameters of thin films of $\text{Ge}_{1-x}\text{Sn}_x\text{Se}_{2.5}$ ($x=0, 0.3, 0.5$) glasses have been investigated using the absorption and transmission data obtained using UV-Vis-NIR spectrophotometer. Data

has been analysed to obtain optical constants such energy band gap, refractive index, extinction coefficient etc. for these samples.

2. Experimental details

Amorphous samples of $\text{Ge}_{1-x}\text{Sn}_x\text{Se}_{2.5}$ ($x=0, 0.3, 0.5$) alloys were prepared using the conventional melt quenching method. High purity (99.999 %) Ge, Sn and Se bought from Sigma Aldrich were used sample preparation. The constituent materials were weighed in appropriate atomic weight percentage and mixed thoroughly using mortar and pestle. This mixture was then transferred to quartz ampoules and these ampoules were further sealed at a vacuum of 10^{-5} Torr. The sealed ampoules were then placed in furnace where they were heated at 1000°C for about 15 hours. The ampoules were rotated frequently to facilitate the homogenization of the sample. The molten samples were quenched in ice-cooled water to get glassy state. The ingots of the ampoules were grinded to powder form using mortar and pestle.

The thin films of samples were deposited onto glass substrate by thermal vacuum evaporation technique. The absorption and transmission spectra in the spectral range 400 – 1200 nm were recorded using a double beam UV-Vis-NIR spectrophotometer (Perkin Elmer, λ 750). All the measurements reported were taken at 300 K.

3. Result and discussion

3.1. Structural characterization

Fig.1 shows the X-ray diffraction patterns of as-prepared $\text{Ge}_{1-x}\text{Sn}_x\text{Se}_{2.5}$ ($x=0, 0.3, 0.5$) glassy alloys. The

absence of any sharp peak in the diffraction patterns confirms the amorphous nature of these samples.

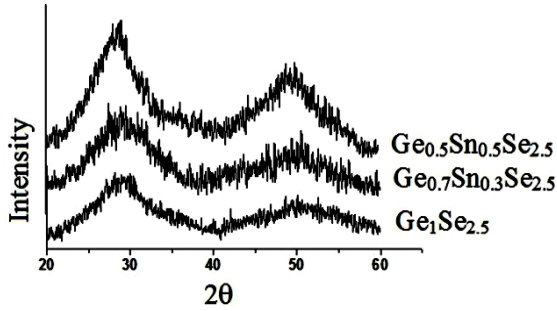


Fig. 1. XRD pattern of the bulk $\text{Ge}_{1-x}\text{Sn}_x\text{Se}_{2.5}$ ($x=0, 0.3, 0.5$) glasses

3.2. Determination of Cohesive energy (C.E), coordination number, $\langle Z \rangle$, heat of atomization (H_s)

Cohesive energy (C.E) of $\text{Ge}_{1-x}\text{Sn}_x\text{Se}_{2.5}$ ($x=0, 0.3, 0.5$) glassy alloys has been calculated using chemical bond approach (CBA) [23]. According to CBA theory, the heteropolar bonds are formed first followed by homopolar bonds. Higher energy bonds are formed first and then bonds are formed in the order of decreasing bond energy until the available valence of the atom is satisfied. Consequently, bonds between like atoms will only occur if there is an excess of certain type of atoms. Besides, the bond energies are assumed to be additive. The bond energies $E(A-B)$ for heteronuclear bonds have been calculated by using the relation [24]:

$$E(A-B) = [E(A-A) \times E(B-B)]^{1/2} + 30[\chi_A - \chi_B]^2 \quad (1)$$

where, χ_A , χ_B , $E(A-A)$ and $E(B-B)$ are the electronegativity and the homopolar bond energies of A and B atoms respectively. The homonuclear bond energies of Ge-Ge, Se-Se and Sn-Sn are 188 kJ/mol, 206.1 kJ/mol and 164.6 kJ/mol respectively [25] and the electronegativity values of Ge-Ge, Se-Se and Sn-Sn are 1.8, 2.4 and 1.9 respectively [26]. The heteronuclear binding energy of Ge-Se and Sn-Se obtained from eq. (1) is 207.6 kJ/mol and 191.6 kJ/mol respectively. The distribution of chemical bonds as obtained from CBA is given in Table 1. Using the values of heteronuclear and homonuclear bond energies, the cohesive energies of the compositions have been calculated by adding up the bond energies of all the bonds expected in the system under study.

The average coordination number for a glassy system $\text{Ge}_x\text{Sn}_y\text{Se}_z$ ($x + y + z = 100$) can be obtained using the following relation [27-28]:

$$\langle Z \rangle = (x\langle Z \rangle_{\text{Ge}} + y\langle Z \rangle_{\text{Sn}} + z\langle Z \rangle_{\text{Se}}) / (x + y + z) \quad (2)$$

where $\langle Z \rangle_{\text{Ge}}$, $\langle Z \rangle_{\text{Sn}}$ and $\langle Z \rangle_{\text{Se}}$ are the co-ordination numbers of Ge, Sn and Se respectively. Table 1 lists the values of the average coordination number. It can be

observed from table 1 that value of coordination number decreases on increase of Sn composition in samples under investigation. A decrease in Z infers that system becomes less connected on increase in Sn content in samples.

Heat of atomization H_s , has been evaluated using from the following relation [29]:

$$H_s = \frac{(\alpha H_s^{\text{Ge}} + \beta H_s^{\text{Sn}} + \gamma H_s^{\text{Se}})}{\alpha + \beta + \gamma} \quad (3)$$

The single value of heat of atomization for Ge, Sn and Se are 433.26, 346.60 and 237.81 kJ/mol respectively [24-25]. The values of H_s are mentioned in Table 1. It is observed that both C.E. and H_s decreases with increase in Sn content in the samples.

This means the average stabilization energy of the glass matrix decreases with increasing concentration of Sn. The decrease in C.E. means decrease in bonding strength of the material. The decrease in H_s also indicates the same fact. The variation of C.E., Z and H_s with Sn content can also be correlated to the optical band gap, E_g , [30-31]. This has been discussed later in this paper.

3.3. Optical parameters

3.3.1. Calculation of refractive index, extinction coefficient and dielectric constant

Fig. 2 shows the transmission spectra in the range 400-1200 nm of the films of $\text{Ge}_{1-x}\text{Sn}_x\text{Se}_{2.5}$ ($x=0, 0.3, 0.5$) glassy alloys. From Fig. 2, it is observed that there is no sharp absorption edge, which indicates the glassy state of samples. The transmission spectra shows emergence of numerous maxima and minima with the increase of wavelength. Therefore, Swanepoel method [32] has been used to calculate the refractive index (n) and thickness (d) of the films from the transmission spectra. This method is based on creating envelopes of interference maxima and minima appearing in the transmission spectrum, for determination of refractive index in weak and medium absorption region ($\alpha \neq 0$).

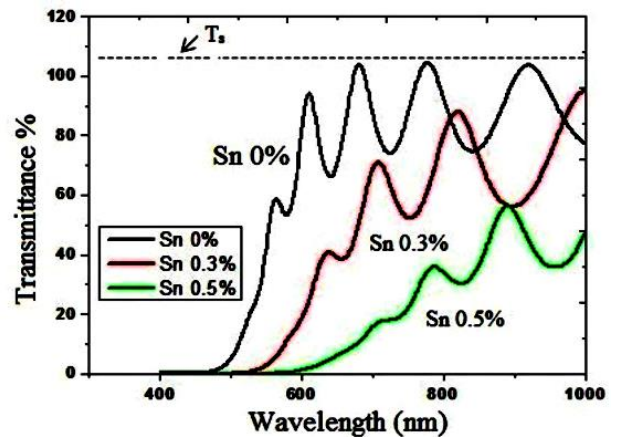


Fig. 2. Transmission spectra of the films of $\text{Ge}_{1-x}\text{Sn}_x\text{Se}_{2.5}$ ($x=0, 0.3, 0.5$) glassy alloys

The value of the refractive index (n) of the film can be evaluated using the following relation:

$$n = [N + (N^2 - n_s^2)^{1/2}]^{1/2} \quad (4)$$

where,

$$N = \frac{2n_s(T_M - T_m)}{T_M T_m} + \frac{n_s^2 + 1}{2} \quad (5)$$

where T_M is the maxima of the upper envelope and T_m is the minima value of lower envelope at a certain wavelength. n_s denote the refractive index of the glass substrate. The refractive index of the glass substrate has been calculated using T_s (transmittance spectra of the glass substrate) from the relation:

$$n_s = \frac{1}{T_s} + \left(\frac{1}{T_s^2} - 1 \right)^{1/2} \quad (6)$$

Table 1. Value of number of chemical bonds, cohesive energy, coordination number and heat of atomization of $Ge_{1-x}Sn_xSe_{2.5}$ ($x=0, 0.3, 0.5$) glasses

Samples	Values of chemical bonds				Physical properties		
	Ge-Se	Sn-Se	Se-Se	Sn-Sn	C.E. (kJ/mol)	$\langle Z \rangle$	H_s (kJ/mol)
$Ge_1Se_{2.5}$	0.326	-	0.674	-	206.5	2.57	293.65
$Ge_{0.7}Sn_{0.3}Se_{2.5}$	0.355	0.145	0.5	-	204.5	2.40	286.22
$Ge_{0.5}Sn_{0.5}Se_{2.5}$	0.422	0.475	-	0.103	195.5	2.28	281.27

The thickness (d) of thin film was evaluated with help of the refractive indices at two adjacent maxima (or minima) respectively n_1 and n_2 at wavelengths λ_1 and λ_2 . Film thickness (d) is obtained using relation,

$$d = \frac{\lambda_1 \lambda_2}{2(\lambda_1 n_2 - \lambda_2 n_1)} \quad (7)$$

The obtained thickness of the film is in the range 400-450 nm.

The variation of refractive index with wavelength is shown in Fig. 3. The values of refractive index obtained for the glass films at wavelength 1000 nm are given in Table 2. From Table 2 and Fig.3, it is observed that refractive index increases with increase in Sn content in

samples. This increase can be attributed to variation of polarizability and refractive index as proposed by Lorentz-Lorenz [33] according to the following expression:

$$\frac{n^2 - 1}{n^2 + 2} = \frac{1}{2\epsilon_0} \sum_j N_j \alpha_{p,j} \quad (8)$$

where ϵ_0 is the vacuum permittivity and N_j is the number of polarizable units of type j per volume unit, with polarizability $\alpha_{p,j}$. The atomic radius of Ge, Se and Sn is 1.22 Å, 1.20 Å and 1.40 Å respectively. Therefore, when Sn replaces Ge site, polarizability increases, consequently refractive index also increases.

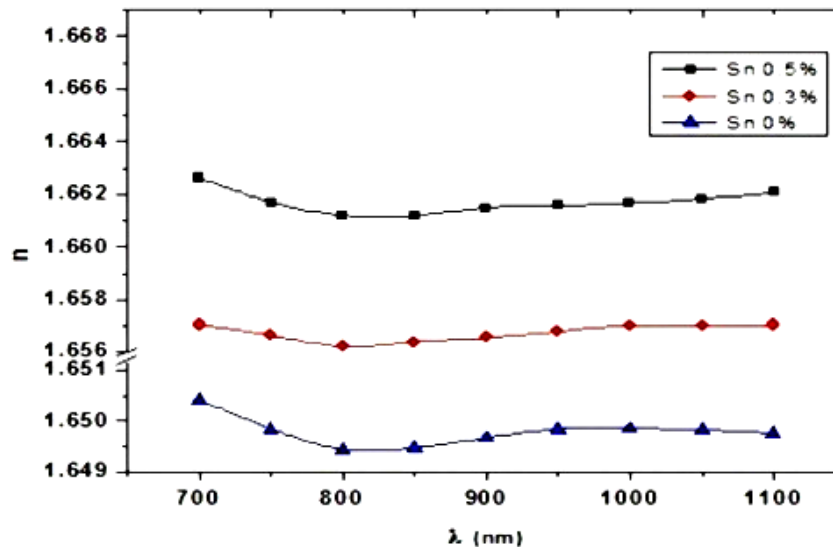


Fig. 3. Variation of refractive index with wavelength for thin films $Ge_{1-x}Sn_xSe_{2.5}$ ($x=0, 0.3, 0.5$) glasses

The value of extinction coefficient, k , can be obtained with the help of absorption coefficient, using the following relation [34]

$$k = \frac{\alpha\lambda}{4\pi} \quad (9)$$

The real and imaginary parts [35] of the dielectric constant ϵ' and ϵ'' can be calculated from the knowledge of refractive index and extinction coefficient from the following expressions

$$\epsilon' = n^2 - k^2 \quad (10)$$

$$\epsilon'' = 2nk \quad (11)$$

The values of extinction coefficient and dielectric constant (real and imaginary) are mentioned in Table 2 at wavelength 1000 nm. It is observed that k , ϵ' and ϵ'' increases with increase of Sn content in samples. The increase these parameters indicate increase in attenuation in electromagnetic wave and permittivity of the samples.

The value of n can be also used to analyse the high frequency dielectric constant (ϵ_∞) by using the following expression [36]

$$n^2 = \epsilon_\infty - \left(\frac{e^2 N}{4\pi c^2 \epsilon_0 m^*} \right) \lambda^2 \quad (12)$$

where ϵ_0 is the vacuum permittivity (8.854×10^{-12} F/m), e is the electronic charge, N is the charge carrier concentration, m^* is the effective mass of the charge carrier and c is the speed of light. The plots of n^2 versus λ^2 for thin films $Ge_{1-x}Sn_xSe_{2.5}$ ($x=0, 0.3, 0.5$) glasses are shown in Fig. 4. The intercept and slope of the plot gives the values of ϵ_∞ and N/m^* respectively. The values of ϵ_∞ and N/m^* are given in Table 2. It is observed that both ϵ_∞ and N/m^* increases with increase in Sn content in the samples. This may be attributed to the increase in free carrier concentration.

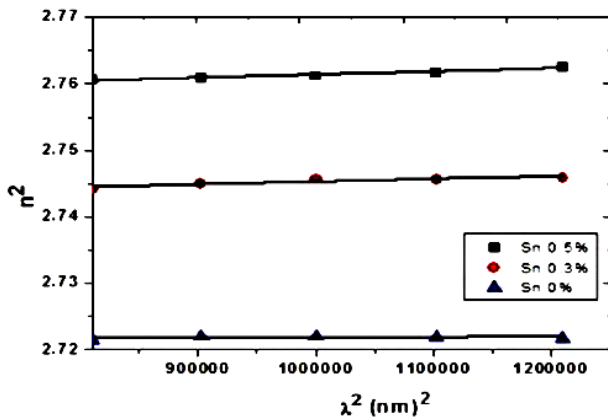


Fig. 4. Plots of n^2 versus λ^2 for thin films $Ge_{1-x}Sn_xSe_{2.5}$ ($x=0, 0.3, 0.5$) glasses

3.3.2. Determination of the absorption coefficient (α) and optical band gap (E_g)

Fig. 5 shows the plots of absorbance versus wavelength for all the samples under investigation in the range 400-1200 nm. The relation between the absorption coefficients (α) and the incident photon energy ($h\nu$) is given by [37-38]:

$$(\alpha h\nu) = A (h\nu - E_g)^n \quad (13)$$

where A is a constant and E_g is the band gap of the material and exponent n depends on the type of transition.

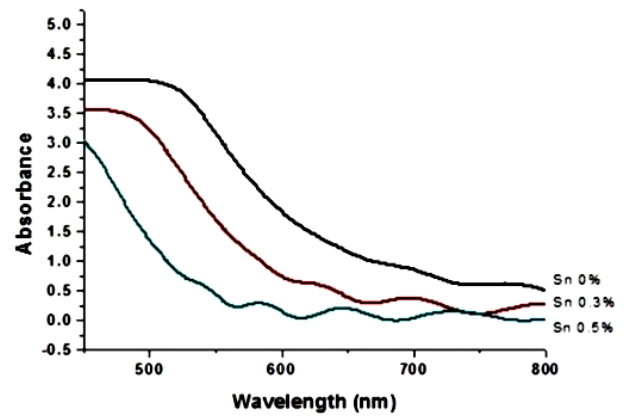


Fig. 5. The absorbance versus wavelength plot for $Ge_{1-x}Sn_xSe_{2.5}$ ($x=0, 0.3, 0.5$) thin films

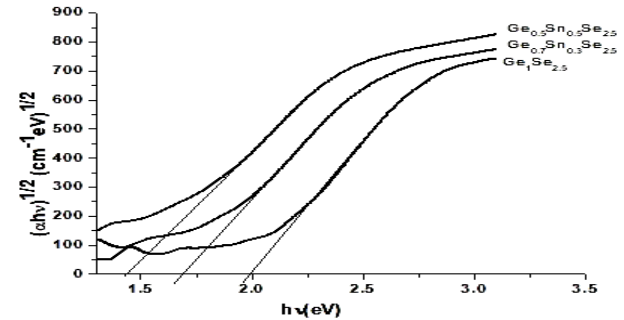


Fig. 6. Plot of $(\alpha h\nu)^{1/2}$ versus $h\nu$ for $Ge_{1-x}Sn_xSe_{2.5}$ ($x=0, 0.3, 0.5$) thin films

The energy band gap is calculated from the absorption spectra by plotting a graph between $(\alpha h\nu)^{1/2}$ and $h\nu$ (Fig. 6). Table 2 lists the values of energy band gap (E_g) for all the samples. The band gap values were found to decrease on increase of Sn composition in the samples. This can be attributed to structure of $Ge_{1-x}Sn_xSe_{2.5}$ glassy system [21]. The glassy state of $GeSe_2$ is built up of $Ge(Se_4)_{1/2}$ tetrahedra, which is cross-linked by edge-sharing bitetrahedra. Randomly-oriented clusters of these are formed which are crosslinked by Se-Se bonds. This system has only Ge-Se and Se-Se bonds.

When Sn is added to GeSe₂ system, it goes substitutionally into Ge sites preferentially occupying the sites at the edges of the clusters [39]. When Sn is added at the cost of Ge, Sn-Se bonds formation take place at the cost of Ge-Se bonds. On further addition of Sn, formation of Sn-Sn bonds also take place along with Sn-Se bonds, which results in decrease of Se-Se bonds. This creates a conformational disorder in the network, which creates additional energy states within the bandgap leading to increase in the density of states near the band. Thus, a decrease in band gap values was observed.

The decrease in band gap, E_g , can also be explained on the basis of physical properties (C.E., $\langle Z \rangle$ etc.) of samples depicted in Table 1. In chalcogenide glasses, the valence band (σ -bonding) originates from lone pair (LP) electron states, whereas, the conduction band arises from anti-bonding (σ^*) states [40-41]. The coordination number ($\langle Z \rangle$), which indicates network connectedness [42], decreases on increase of Sn concentration. This suggest that interaction between the atomic species decreases which inturn narrows the gap between σ and σ^* states, consequently decreasing the energy band gap (E_g) of the samples. Moreover, the decrease in C.E. of Ge-Sn-Se system tends to decrease the energy of the conduction band edge causing a lesser gap between σ and σ^* orbitals and thus resulting in observed decrease in band gap (E_g).

The absorption coefficient depends exponentially on the photon energy as given by the empirical relation [43]:

$$\ln \alpha = \ln B + \left(\frac{h\nu}{E_c} \right) \quad (14)$$

where E_c is Urbach energy and corresponds to the band tail width which generally characterizes the degree of disorder in an amorphous semiconductor [44] and B is a constant. The variation of $\ln(\alpha)$ with $h\nu$ is depicted in Fig. 7.

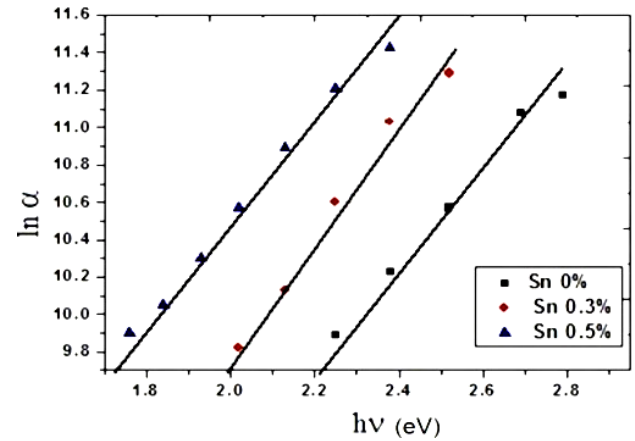


Fig. 7. Variation of $\ln \alpha$ vs photon energy for thin films $Ge_{1-x}Sn_xSe_{2.5}$ ($x=0, 0.3, 0.5$) glasses

Table 2. Values of energy band gap (E_g), refractive index (n), extinction coefficient (k), dielectric constant (real ϵ' and imaginary ϵ''), high frequency dielectric constant (ϵ_∞) and N/m^* of $Ge_{1-x}Sn_xSe_{2.5}$ ($x=0, 0.3, 0.5$) thin films

Sample	E_g (eV)	n (at $\lambda=1000$ nm)	k (at $\lambda=1000$ nm)	E_c	ϵ' (at $\lambda=1000$ nm)	ϵ'' (at $\lambda=1000$ nm)	ϵ_∞	N/m^*
$Ge_1Se_{2.5}$	1.98	1.64	0.04	0.29	2.71	0.15	2.72	0.22×10^{36}
$Ge_{0.7}Sn_{0.3}Se_{2.5}$	1.67	1.65	0.07	0.32	2.73	0.25	2.74	1.50×10^{36}
$Ge_{0.5}Sn_{0.5}Se_{2.5}$	1.43	1.66	0.09	0.38	2.75	0.31	2.75	1.86×10^{36}

It is observed that absorption coefficient varies linearly with photon energy, which is in accordance with the Urbach rule. The inverse of slope of straight line gives the values of E_c at different Sn compositions. These values are tabulated in Table 2. Urbach energy (E_c) was found to increase on increasing Sn percentage in samples. This may be due to accumulation of atoms on the surface of substrate, which may cause the formation of structural defects. These defects and degree of disorder together affects the width of localised states near the mobility edge. These defects can introduce localized states near the band edges resulting in decrease of band gap [45]. Thus an increase in E_c with Sn content support the decrease observed in the band gap of the samples with increasing Sn content.

4. Conclusions

The present paper reports the study of optical and dispersion properties of thin films of $Ge_{1-x}Sn_xSe_{2.5}$ ($x=0, 0.3, 0.5$) glassy alloys. The XRD pattern shows that bulk samples are amorphous in nature. It is found that the optical band gap (E_g) decreases with increase in Sn content in the samples. This decrease is attributed to the increase in density of states (E_c) near the band edges. The physical properties C.E., $\langle Z \rangle$ and H_s also supports this fact. The decrease in C.E. of Ge-Sn-Se system tends to decrease the energy of the conduction band edge causing a lesser gap between σ and σ^* orbitals and thus resulting in observed decrease in band gap (E_g).

Further, it was observed that the values of refractive index (n) increases with increase of Sn content in the samples. The increase in n is due to increase in polarizability of atoms on replacing Ge with Sn atoms. The Urbach energy (E_c) was found to increase on increasing Sn percentage in samples. This may be due to accumulation of atoms on the surface of substrate, which may cause the formation of structural defects. The increase in E_c with Sn content support the decrease observed in the band gap of the samples with increasing Sn content.

The decreased value of band gap makes Ge_{0.5}Sn_{0.5}Se_{2.5} glass ideal for opto-electronic devices.

Acknowledgements

First author Deepika is highly thankful to the Department of Science and Technology, Government of India for financial support vide reference no.SR/WOS-A/PM-1017/2014 under Women Scientist Scheme to carry out this work.

References

- [1] A. B. Seddon, M. J. Laine, *J. Non-Cryst. Solids* **213-214**, 168 (1997).
- [2] G. F. Zhou, *Mater. Sci. Engg. A* **304-306**, 73 (2001).
- [3] Deepika, H. Singh, K. S. Rathore, N. S. Saxena, *Adv. Sci. Lett.* **22**, 3940 (2016).
- [4] M. Ghayebloo, M. Rezvani, M. Tavoosi, *Infrared Physics & Technology* **90**, 40 (2018).
- [5] R. I. Alekberov, A. I. Isayev, S. I. Mekhtiyeva, M. Fábían, *Physica B* **550**, 367 (2018).
- [6] Pawan Kumar, S.K. Tripathi, I. Sharma, *Journal of Alloys and Compounds* **755**, 108 (2018).
- [7] J. Tauc, *Amorphous and liquid semiconductors*, Plenum Press, New York, 1974.
- [8] A. E. Owen, A. P. Firth, P. J. S. Ewen, *Phil. Mag. B* **52**, 347 (1985).
- [9] T. S. Moss, *Optical properties of semiconductors*, Butterworths, London, 1959.
- [10] Y. Tawada, K. Tsuge, M. Kondo, H. Okamoto, Y. Hamakawa, *J. Appl. Phys.* **53**, 5273 (1982).
- [11] H. Wang, F. Gan, J. Fusung, *J. Non Cryst. Solids* **112**, 291 (1989).
- [12] S. H. Lee, Y. Jung, H. S. Chung, A. T. Jennings, R. Agarwal, *Physica E: Low-dimens. Syst. Nanostruct.* **40**, 2474 (2008).
- [13] M. De Sario, L. Mescia, F. Prudenzeno, F. Smektala, F. Deseveday, V. Nazabal, J. Troles, L. Brilland, *Optics & Laser Technol.* **41**, 99 (2009).
- [14] L. Brus, *Appl. Phys. A* **53**, 465 (1991).
- [15] P. Boolchand, J. Grothaus, W. J. Bresser, P. Suranyi, *Phys. Rev. B* **25**(4), 2975 (1982).
- [16] N. A. Jemalim, H. A. Kassim, V. R. Devi, K. N. Shrivastava, *J. Non-Cryst. Solids* **354**, 1744 (2008).
- [17] K. Sedeek, A. Adam, M. R. Balboul, L. A. Wahab, N. Makram, *Mater. Res. Bull.* **43**, 1355 (2008).
- [18] Y. Murakami, T. Usuki, M. Sakurai, S. Kohara, *Mater. Sci. Engg. A* **449-451**, 544 (2007).
- [19] C. R. Schardt, J. H. Simmons, P. Lucas, L. Le Neindre, J. Lucas, *J. Non-Cryst. Solids* **274**, 23 (2000).
- [20] D. J. Sarrach, J. P. de Neufville, W. L. Hawoth, *J. Non-Cryst. Solids* **22**, 245 (1976).
- [21] Deepika, K. S. Rathore, N. S. Saxena, *J. Phys. Condens. Matter* **21**, 335102 (2009).
- [22] Deepika, P. K. Jain, K. S. Rathore, N. S. Saxena, *Phil. Mag. Letters* **89**(3), 194 (2009).
- [23] J. Bicerano, S. R. Ovshinsky, *J. Non-Cryst. Solids* **74**, 75 (1985).
- [24] L. Pauling, *The Nature of the Chemical Bond*, Third ed. Cornell University Press, New York, 1960.
- [25] Deepika, K. S. Rathore, N. S. Saxena, *J. Therm. Anal. Calorim.* **98**, 725 (2009).
- [26] H. M. Kotb, F. Abdel-Rahim, *Mater. Sci. Semiconduct. Process.* **38**, 209 (2015).
- [27] Deepika, H. Singh, N. S. Saxena, *Trans. Ind. Ceram. Soc.* **75**, 20 (2016).
- [28] P. Bavafa, M. Rezvani, *Results in Physics* **10**, 777 (2018).
- [29] E. R. Shaaban, *J. Phys. Chem. Solids.* **68**, 400 (2007).
- [30] A. Kaistha, V. R. Rangra, P. Sharma, *Glass Phys. Chem.* **41**, 175 (2015).
- [31] A. El-Korashy, N. El-Kabany, H. El-Zahed, *Physica B* **365**, 55 (2005).
- [32] R. Swanepoel, *J. Phys. E: Sci. Instrum.* **16**, 1214 (1983).
- [33] Deepika, H. Singh, *Nano-struct. and Nano-objects* **10**, 192 (2017).
- [34] S. Ahmadpour, M. Rezvani, P. Bavafa, *Spectrochimica Acta Part A: Molecular and Biomolecular Spectroscopy* **205**, 258 (2018).
- [35] T. S. Moss, G. J. Burrell, E. Ellis, *Semiconductor Opto-electronics*, Butterworths, London, 1973.
- [36] Deepika, H. Singh, *Infrared Phys. Technol.* **85**, 39 (2017).
- [37] K. S. Rathore, Deepika, D. Patidar, N. S. Saxena, K. B. Sharma, *J. Ovon. Res.* **5**, 175 (2009).
- [38] K. S. Rathore, Y. Janu, Deepika, K. Sharma, N. S. Saxena, *Optoelectron. Adv. Mater.* **3**(4), 313 (2009).
- [39] S. A. Fayek, M. H. Ali, *J. Mater. Sci.* **30**, 2838 (1995).
- [40] M. Kastner, *Phys. Rev. Lett.* **28**, 355 (1972).
- [41] G. Saffarini, J. M. Saiter, H. Schmitt, *Optical Materials* **29**, 1143 (2007).
- [42] J. P. De Neufville, H. Rockstad, J. Stuke, W. Bernig (Eds.), *Amorphous and liquid semiconductors*, Taylor and Francis, London, 1974.
- [43] F. Urbach, *Phys. Rev.* **92**, 1324 (1953).
- [44] M. M. Abdel-Aziz, E. G. El-Metwally, M. Fadel, H. H. Labib, M. A. Afifi, *Thin Solid Films* **386**, 99 (2001).
- [45] N. F. Mott, E. A. Davis, *Electronic Processes in Non-Crystalline Materials*, Clarendon Press, Oxford, 1979.

*Corresponding author: deepika.spsl@gmail.com